Journal of Innovative Optical Health Sciences
Vol. 9, No. 2 (2016) 1650005 (6 pages)

DOI: 10.1142/S179354581650005X

World Scientific
www.worldscientific.com

Change of photosensitizer fluorescence at its diffusion in viscous liquid flow

Valeriya S. Maryakhina* and Vyacheslav V. Gun'kov
Orenburg State University
13 Pobedy st., Orenburg 460018, Russia
**v.s.maryakhina@gmail.com*

Received 17 May 2015
Accepted 29 June 2015
Published 13 August 2015

In this paper, the mathematical model of distribution of the injected compound in biological liquid flow has been described. It is considered that biological liquid contains a few phases such as water, peptides and cells. The injected compound (for example, photosensitizer) can interact with peptides and cells. At the time, viscosity of the biological liquid depends on pathology present in organism. The obtained distribution of the compound connects on changes of its fluorescence spectra which are registered during fluorescent diagnostics of tumors. It is obtained that the curves do not have monotonic nature. There is a sharp curves decline in the first few seconds after injection. Intensivity of curves rises after decreasing. It is especially pronounced for wavelength 590 nm and 580 nm (near the "transparency window" of biological tissues). Time of inflection point shifts from 8.4 s to 6.9 s for longer wavelength. However, difference between curves is little for different viscosity means of the biological liquid. Thus, additional pathology present in organism does not impact to the results of *in vivo* biomedical investigations.

Keywords: Fluorescence; diffusion; biomedical diagnostics; photosensitizer; viscosity.

1. Introduction

For fluorescent diagnostics of cancer diseases photosensitizer would be injected in biological liquid (blood as a rule). Photosensitizer molecules penetrate into biological structures diffused in flow. The selective accumulation of photosensitizer molecule in cancer cells is as a result of diffusion process. It leads to some fluorescence spectrum change in which emission of the immobilized and free-diffused molecules in water medium is included. However, calculation of part of the photosensitizer connected on biostructures and free diffused is difficult.

In this paper, we discuss influence of blood viscosity on the results of measurements of fluorescence spectra and, as a consequence, of optical biomedical diagnostics of tumors.

2. Experimental Research

The object of the experimental research was bengal rose ($M = 832.4\,\mathrm{g/mol}$). It is one of xanthene dyes

used in biomedical research. It was shown earlier[1] that bengal rose penetrates into cells located in cytoplasm and connects on peptides, at this time bengal rose interests as a photosensitizer.[2]

Solutions of bengal rose dissolved in phosphate buffer (pH = 7.4), blood serum albumin (concentration 8% (weight)) and suspension of cancer mammary cells of BYRB mice line prepared for method[3] were used as a model media. For spectral measurements the obtained cell suspension was centrifuged at 4000 min^{-1} 5 min with supernatant removal and next addition of phosphate buffer. The procedure was repeated twice. Concentration of bengal rose in all samples was $0.5 \cdot 10^{-4}$ M for exclusion of concentration effect.[4] Fluorescence spectra of photosensitizer in three media were measured on the fluorimetric setup described in our previous work.[5] 510 nm is the excitation wavelength.

In Fig. 1, fluorescence spectra of bengal rose dissolved in phosphate buffer, blood serum albumin and suspension of the life cancer mammary cells are represented. It is shown that fluorescence spectra of bengal rose dissolved in biological objects shifts to long wave region relatively to dye fluorescence in buffer solution. Width of the fluorescence spectra rises from 30 nm (Curve 1) to 38 nm (Curves 2 and 3). This dependence was also shown by other authors.[6–8] The obtained result can be explained by immobilization of the dye in biological structures. Since photosensitizer can be injected in either unmovable or movable medium, rate of immobilization processes depend on medium rate. The results of the theoretical researches of the phenomenon are described in the next section of the paper.

3. The Mathematical Model

In this paper, we will describe system in which compound source is instantaneous. The compound is injected in biological liquid flow contained a few phases such as water phase, phase of biological active molecules (peptides, enzymes) and cell phase (erythrocytes, somatic cells, bacteria). The investigated compound can penetrate into these structures and fluorescent inside. It is considered in the model that no chemical reactions occur; physical interactions of the compound with these structures proceed only. While these interactions are strong, decay of the complex (photosensitizer-peptide and photosensitizer-cells) formed at the experiment time does not occur. Thus, these biostructures are "traps" for the injected compound.

There is a great variety of absorbing components in biological systems; their reactivity is mainly determined by the radius and volume concentration. Despite of the heterogeneity of the surface and shape of the biological structures, we assume that they have spherical form and are uniformly localized throughout the volume. In this paper, we will consider two types of absorbent components which are greatly different from each other for diameter and

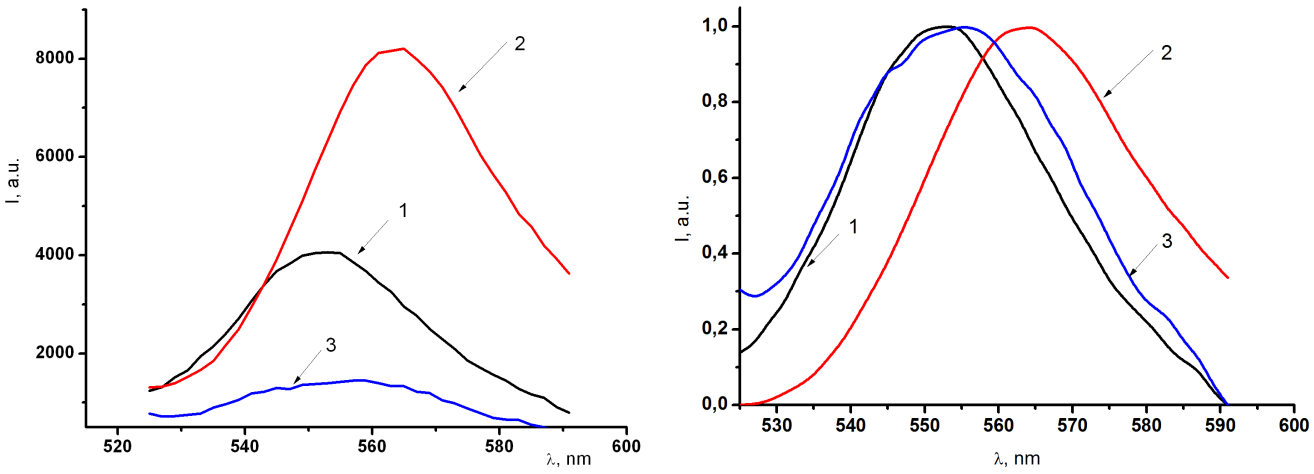

Fig. 1. Fluorescence spectra of bengal rose in: 1 — buffer solution, 2 — in blood serum albumin, 3 — cancer mammary cells suspension, (a) native spectra and (b) normalized spectra.

concentration. Concentration of the first type of biological structures (peptide phase) will be designated as $C_p(t)$, concentration of the second type (cell phase) will be designated as $C_{\text{cell}}(t)$.

We will consider diffusion in the moved biological liquid flow. Therefore, the kinetic equations were based on the transport equation

$$\frac{\partial C(r,t)}{\partial t} + \bar{w}\text{grad}C = D\nabla^2 C(r,t).$$

Since the described biological medium is movable, the concentration distribution of the injected substances in any section will depend on the time. But each particular section can be separated in the spherical form. Therefore, the task can be regarded as spherical symmetry due to the assumption of uniform distribution of "traps" in space. Then we can write the Laplacian in spherical coordinates without dependence φ and θ.

Taking into account this assumption, the kinetic equations for each phases are given as

$$\begin{cases} \dfrac{\partial C_w(r,t)}{\partial t} + \overline{w}_w \dfrac{\partial C_w(r,t)}{\partial r} \\ \quad = D_w\left(\dfrac{\partial^2 C_w(r,t)}{\partial r^2} + \dfrac{1}{r}\dfrac{\partial C_w(r,t)}{\partial r}\right) \\ \quad - k_1 C_w(r,t)C_p(r,t) - k_2 C_w(r,t)C_{\text{cell}}(r,t), \\ \dfrac{\partial C_p(r,t)}{\partial t} + \overline{w}_p \dfrac{\partial C_p(r,t)}{\partial r} \\ \quad = D_p\left(\dfrac{\partial^2 C_p(r,t)}{\partial r^2} + \dfrac{1}{r}\dfrac{\partial C_p(r,t)}{\partial r}\right) \\ \quad - k_1 C_w(r,t)C_p(r,t), \\ \dfrac{\partial C_{\text{cell}}(r,t)}{\partial t} + \overline{w}_{\text{cell}} \dfrac{\partial C_{\text{cell}}(r,t)}{\partial r} \\ \quad = D_{\text{cell}}\left(\dfrac{\partial^2 C_{\text{cell}}(r,t)}{\partial r^2} + \dfrac{1}{r}\dfrac{\partial C_{\text{cell}}(r,t)}{\partial r}\right) \\ \quad - k_2 C_w(r,t)C_{\text{cell}}(r,t). \end{cases}$$

Rates of all phases have their own profile. In present calculations, we will use average rate mean. It is shown[9] that rates of cells and plasma are different. For decision of the system we assume that all phases rate are equal, that is, $w_w = w_p = w_{\text{cell}}$. Next, change of variables $x = r + wt$ can be carried out. In the case the equation system is reduced to decision of diffusion equation system

$$\begin{cases} \dfrac{\partial C_w(x,t)}{\partial t} = D_w\left(\dfrac{\partial^2 C_w(x,t)}{\partial x^2}\right) - k_1 C_w(x,t)C_p(x,t) \\ \quad - k_2 C_w(x,t)C_{\text{cell}}(x,t), \\ \dfrac{\partial C_p(x,t)}{\partial t} = D_p\left(\dfrac{\partial^2 C_p(x,t)}{\partial x^2}\right) - k_1 C_w(x,t)C_p(x,t), \\ \dfrac{\partial C_{\text{cell}}(x,t)}{\partial t} = D_{\text{cell}}\left(\dfrac{\partial^2 C_{\text{cell}}(x,t)}{\partial x^2}\right) \\ \quad - k_2 C_w(x,t)C_{\text{cell}}(x,t). \end{cases} \quad (1)$$

For decision of the system (1) the diffusion coefficient for each of the phases needs to calculate in according to the Einstein–Smolukhovsky law

$$D = \frac{kT}{6\pi\eta R},$$

where k — Boltzman constant, T — temperature, K; η — medium viscosity, Pz; R — radius, m.

We are taking into account that temperature for biological media is 310 K, average of peptide size is 40 nm, average cell size is 25 mkm. In this paper, we assume that blood viscosity mean is from 0.2 cPz to 1 cPz.[10] Diffusion coefficients for each phase are different for each viscosity mean.

Equation for rate constant k_i can be written[11] assuming that limiting process of interaction of the investigated compound with biological liquid is diffusion

$$k_i = \frac{2kT}{3\eta} \cdot \frac{R_i + R}{R_i \cdot R}, \quad (2)$$

where R_i — peptides/cells size, nm; R — size of the injected compound molecule, nm.

4. Initial Conditions

For decision of the system (1) the initial conditions need to know. For that we assume that vessel diameter is 0.5 cm and the injected compound is a water solution. Thus, distribution of its concentration can be described by Gauss function with half-width 0.5 mm.

Molecule size of peptides and cells for space are different. For calculations we will use volume concentration value (volume of each phase), that is, multiplication of molecule quantity N to one

molecule volume V_1 the same as we used it in our previous work.[12] It allows to rid the variations of sizes and real number of particles in biological liquid at the evaluation of their concentrations.

It is known[13] that plasma is 60% from blood volume; different cell types are the rest 40% while peptide molecules are 8% in plasma. Finally, we can calculate that 0.6 cm^3 plasma is contained in 1 cm^3 blood and peptide phase volume is given as

$$V_p = 0.6 \cdot 0.08 = 0.048\,\mathrm{cm}^3.$$

Consequently, water phase volume is

$$V_w = 0.6 - 0.048 = 0.552\,\mathrm{cm}^3$$

and cell phase volume

$$V_{\mathrm{cell}} = 1 - 0.048 - 0.552 = 0.4\,\mathrm{cm}^3.$$

Finally, the initial conditions for each phase can be written taking account of their volume ratio

$$C_w(x,0) = 0.552 \cdot \text{Gauss function},$$
$$C_p(x,0) = 0.048,$$
$$C_{\mathrm{cell}}(x,0) = 0.4.$$

5. The Results and Discussion

Compound is redistributed in all volume in the result of diffusion. Integration of $Ci(x,t)$ functions lets us to obtain mean of the reduced compound concentration at each time moment in each phase as

$$C_i(t) = \int_0^{+\infty} C_i(x,t)dx. \tag{3}$$

Quantity of the immobilized molecules of photosensitizer located in peptide and cell phase can be found as

$$C'_p(t) = C_p(0) - C_p(t),$$
$$C'_{\mathrm{cell}}(t) = C_{\mathrm{cell}}(0) - C_{\mathrm{cell}}(t).$$

Changes of the reduced concentration of the investigated compound in free and connected state are depicted in Fig. 2.

The curves for the water phase decrease sharply during the first 8–9 s, and then there is a smooth and slow decline after sharp decreasing. Curves for the immobilized photosensitizer in cells have similar type. However, the curves of peptide phase have more smooth type without inflexions. Thus, the most probable process immediately after injection is its penetration into cells located near injection source. Next, interaction of the photosensitizer is

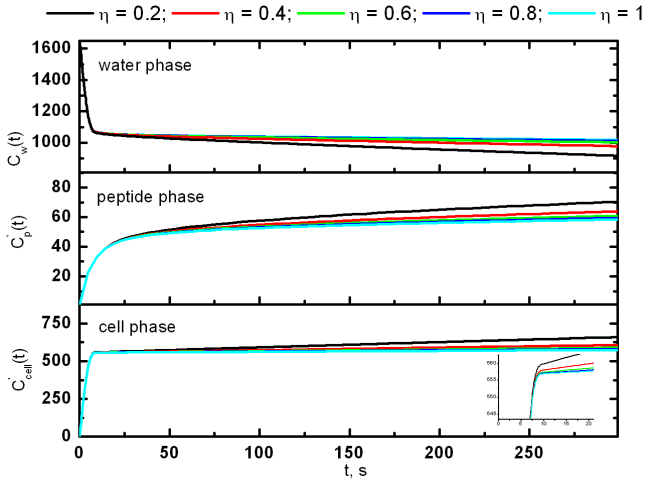

Fig. 2. The kinetic curves of the injected compound concentrations in water, cells and peptide phases for different viscosity means η (from 0.2 cPz to 1 cPz).

with diffused peptide and cells. However, diffuse equilibrium state does not achieve even after 8 min. We note that curves are significantly different for viscosities 0.2 cPz and 0.4 cPz. Further increasing viscosity does not lead to significant difference of curves.

The calculated concentrations $C_i(t)$ for Eq. (3) let to connect quantity of the immobilized compound with changes of fluorescence spectra during time. For that the experimental fluorescence spectra of photosensitizer depicted in Fig. 1 were used. Calculation of spectra dynamics was carried out by formulae

$$S(\lambda) = S_1(\lambda)C_w(t) + S_2(\lambda)C'_p(t) + S_3(\lambda)C'_{\mathrm{cell}}(t), \tag{4}$$

where λ — wavelength, nm; $S(\lambda)$ — final fluorescence spectrum of photosensitizer in the investigated system; $S_1(\lambda)$, $S_2(\lambda)$, $S_3(\lambda)$ — fluorescence spectra of the injected compound concentrations in water, peptide and cells phases, respectively.

The change of final fluorescence spectrum of bengal rose is represented in Fig. 3. As you can see from figure, most change of final spectrum is during the first few seconds. Over time, the spectra are broadened and shifted to longer wavelengths. For detail analysis of fluorescence spectra the graphs of fluorescence intensity change were fitted (Fig. 4). These curves are interesting because fluorescence intensity at one wavelength is measured during

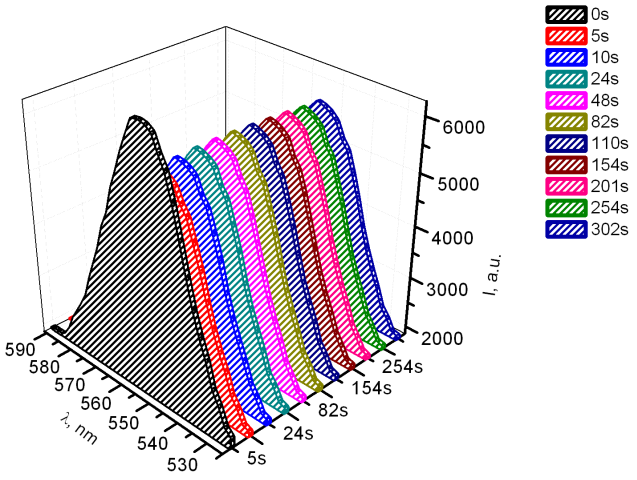

Fig. 3. Dynamics of fluorescence spectra change of bengal rose. Wavelength of excitation is 515 nm. Spectrum was calculate for condition $C_{\text{cell}}(x, 0) = 0.4$.

experimental research. Emission registration are often carried out in the area of 600–650 nm ("transparency window" of tissues). After this we can conclude about accumulation of photosensitizer

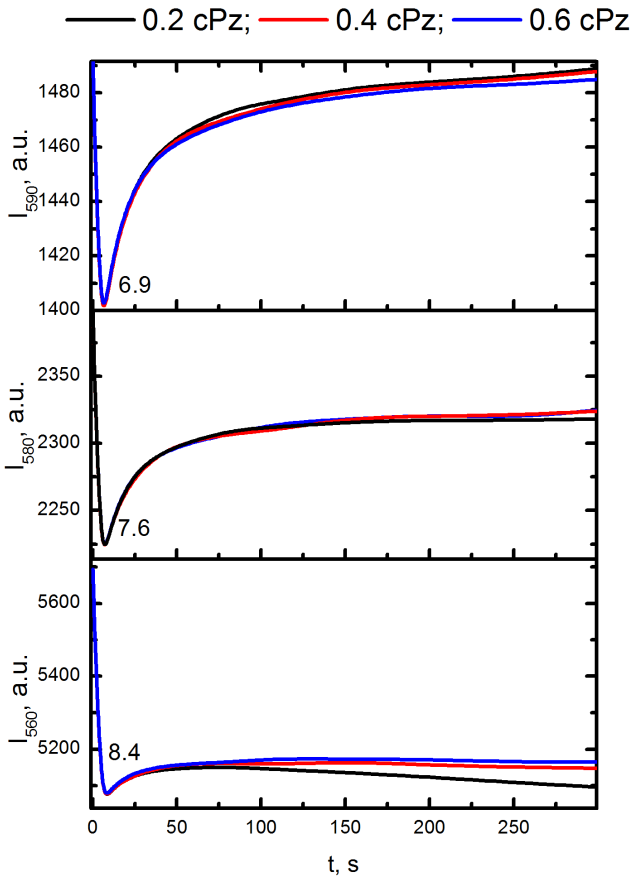

Fig. 4. Changes of bengal rose fluorescence spectrum intensity at 560, 590 and 580 nm to time.

in cancer cells or other biological structures (see Ref. 14).

As you can see from Fig. 4, the curves do not have monotonic nature. There is a sharp curves decline in the first few seconds. Curves intensivity rises after their decreasing. It is especially pronounced for 590 nm and 580 nm (near the "transparency window" of biological tissues). Time of inflection point shifts from 8.4 s to 6.9 s for longer waves. It can be described by photosensitizer immobilization into cells in the first time because of cells large size. It leads to fluorescence extinguishing in according to spectrum 2 in Fig. 1. Next, free-diffused photosensitizer molecules are immobilized into peptides. This process leads to raise fluorescence intensity (in according to spectrum 3 in Fig. 1). However, difference between curves is small for different viscosity means of the biological liquid. Thus, additional pathology present in organism does not impact to the results of *in vivo* biomedical investigations. Increase of luminescence in the first few minutes had been described by researchers of various groups.[15,16] It is concluded that the calculated curves are well agreed with experimental data and, moreover, help to describe gradual immobilization of the used photosensitizer to peptide and cell structures of biological liquid.

6. Conclusion

In this paper, we have described change of fluorescence spectra of the injected compound in biological liquid flow. Really, this model cannot consider processes occurring in all vessel networks. However, it is obtained by the model that the most significant changes of the immobilization process and fluorescence spectra are during the first 6–8 s. After that processes are happening much slower. The time of diffuse equilibrium achievement depends on biological functions of compound and its type. It is considered that blood flow rate in vessel with diameter 0.5 cm is 10 cm/s (Ref. 17) then the injected compound will traverse the path 60–80 cm during 6–8 s. It is an average length of hand. Measurement of fluorescence intensity at longer time region need to consider all vessel networks with its diameter change but the obtained result is important for pharmacokinetics and preparations delivery. Absence of curves dependency on viscosity lets to ignore other pathologies at tumor fluorescence diagnostics. It can be also used for investigation of

photosensitizer interaction with blood flow. Technical scheme of modern experimental devices is often included biological liquid flow where the model can also be used.

Acknowledgment

The work was supported by RFBR grant 14-01-31081 mol_a and president scholarship SP-273.2015.4.

References

1. G. E. Dobretsov, *Fluorescent Probes in Investigation of Cells, Membranes and Lipoproteins*, Science, Moscow (1989).
2. L. Cronin, M. Moffitt, D. Mawad, O. C. Morton, A. Lauto, C. Stack, "An *in vitro* study of the photodynamic effect of rose bengal on trichophyton rubrum," *J. Biophotonics* **7**, 410–417 (2014).
3. V. S. Maryakhina, S. N. Letuta, "Pathology development stage and its influence on the delayed fluorescence kinetics of molecular probes," *Laser Phys.* **23**, 025604 (2013).
4. V. S. Maryakhina, S. N. Letuta, "Concentration of photosensitizers as a factor impacting on the results of fluorescent diagnostics," *Laser Phys.* **24**, 035601 (2014).
5. V. S. Maryakhina, L. S. Scheglova, K. A. Anenkova, "Change of optical properties of hair cells during malignant tumor development," *J. Biomed. Photon. Eng.* **1**, 59–63 (2015).
6. P. F. C. Menezes, C. Bernal, H. Imasato, V. S. Bagnato, J. R. Perussl, "Photodynamic activity of different dyes," *Laser Phys.* **17**, 468 (2007).
7. I. M. Vlasova, A. M. Saletsky, "Raman spectroscopy in comparative investigations of mechanisms of binding of three molecular probes–fluorescein, eosin, and erythrosin–to human serum albumin," *Laser Phys. Lett.* **5**, 834 (2008).
8. A. Penzkofer, A. Tyagi, E. Slyusareva, A. Sizykh, "Phosphorescence and delayed fluorescence properties of fluorone dyes in bio-related films," *Chem. Phys.* **378**, 58–65 (2010).
9. A. R. Pries, T. W. Secomb, "Blood flow in microvascular networks," in *Handbook of Physiology: Microcirculation*, R. F. Tuma, W. N. Dura, K. Ley eds., pp. 3–36, Academic Press (2008).
10. D. S. Long, M. L. Smith, A. R. Pries, K. Ley, E. R. Damiano, "Microviscometry reveals reduced blood viscosity and altered shear rate and shear stress profiles in microvessels after hemodilution," *Proc. Natl. Acad. Sci. USA* **101**, 10060–10065 (2004).
11. N. M. Emanuel', D. G. Knorre, *Course of Chemical Kinetics*, High school, Moscow (1984).
12. V. S. Maryakhina, V. V. Gun'kov, "Fluorescent probe immobilization into enzyme molecules," *Comput. Res. Model.* **5**, 835–843 (2013).
13. D. B. Dill, D. L. Costill, "Calculation of percentage changes in volumes of blood, plasma, and red cells in dehydration," *J. Appl. Physiol.* **37**, 247–248 (1974).
14. L. Tinghui, H. Xiaobin, D. Hong, Z. Jingquan, H. Naiyan, Z. Jing, C. Hongxia, G. Ying, "Liposomal hypocrellin B as a potential photosensitizer for age-related macular degeneration: pharmacokinetics, photodynamic efficacy, and skin phototoxicity *in vivo*," *Photochem. Photobiol. Sci.* **14**, 972–981 (2015).
15. Ch. Perlitz, K. Licha, F.-D. Scholle, B. Ebert, M. Bahner, P. Hauff, K. Th. Moesta, M. Schirner, "Comparison of two tricarbocyanine-based dyes for fluorescence optical imaging," *J. Fluorescence* **15**, 443–454 (2005).
16. M. V. Shirmanova, I. V. Balalaeva, M. A. Sirotkina, N. Y. Lekanova, I. V. Turchin, E. V. Zagaynova, "Study of photosensitizers pharmacokinetics in mouse tumor model by transillumination fluorescence imaging *in vivo*," *Proc. SPIE* **7886**, 78860U–8 (2011).
17. V. A. Levtov, S. A. Regirer, N. H. Shadrina, *Rheology of Blood*, Medicine, Moscow (1982).